Am J Physiol Heart Circ Physiol 299: H1875–H1883, 2010.
First published September 17, 2010; doi:10.1152/ajpheart.00872.2009.

Time course of carotid artery growth and remodeling in response to altered pulsatility

John F. Eberth,[1] Natasa Popovic,[2] Vincent C. Gresham,[3] Emily Wilson,[2] and Jay D. Humphrey[4]

[1]*Department of Engineering Technology, University of Houston, Houston;* [2]*Department of Systems Biology and Translational Medicine,* [3]*Comparative Medicine Program, and* [4]*Department of Biomedical Engineering, Texas A&M University, College Station, Texas*

Submitted 16 September 2009; accepted in final form 10 September 2010

Eberth JF, Popovic N, Gresham VC, Wilson E, Humphrey JD. Time course of carotid artery growth and remodeling in response to altered pulsatility. *Am J Physiol Heart Circ Physiol* 299: H1875–H1883, 2010. First published September 17, 2010; doi:10.1152/ajpheart.00872.2009.—Elucidating early time courses of biomechanical responses by arteries to altered mechanical stimuli is paramount to understanding and eventually predicting long-term adaptations. In a previous study, we reported marked long-term (at 35–56 days) consequences of increased pulsatile hemodynamics on arterial structure and mechanics. Motivated by those findings, we focus herein on arterial responses over shorter periods (at 7, 10, and 14 days) following placement of a constrictive band on the aortic arch between the innominate and left carotid arteries of wild-type mice, which significantly increases pulsatility in the right carotid artery. We quantified hemodynamics in vivo using noninvasive ultrasound and measured wall properties and composition in vitro using biaxial mechanical testing and standard (immuno)histology. Compared with both baseline carotid arteries and left carotids after banding, right carotids after banding experienced a significant increase in both pulse pressure, which peaked at *day 7*, and a pulsatility index for velocity, which continued to rise over the 42-day study despite a transient increase in mean flow that peaked at *day 7*. Wall thickness and inner diameter also increased significantly in the right carotids, both peaking at *day 14*, with an associated marked early reduction in the in vivo axial stretch and a persistent decrease in smooth muscle contractility. Glycosaminoglycan content also increased within the wall, peaking at *day 14*, whereas increases in monocyte chemoattractant protein-1 activity and the collagen-to-elastin ratio continued to rise. These findings confirm that pulsatility is an important modulator of wall geometry, structure, and properties but reveal different early time courses for different microscopic and macroscopic metrics, presumably due to the separate degrees of influence of pressure and flow.

pulse pressure; mouse aortic banding model; hypertension; cyclic strain; mechanics

TIME-DEPENDENT RESPONSES of the arterial system to alterations in local mechanical stimuli result from complex interactions between effectors (e.g., blood pressure and flow) and sensors (mechanosensitive cells). The intricacy of these relationships is compounded by the cyclic nature of the hemodynamic loads experienced in vivo, for these stimuli can have both steady and unsteady components with varying frequencies (14); in the case of flow, there is also potential for reversal (42). Compensatory changes in cellular distribution and extracellular matrix (ECM) composition in response to altered mechanical stimuli are fundamental to both cardiovascular physiology and pathophysiology (2, 11, 15). In fact, evidence suggests that pulse pressure should now be considered an important, independent indicator or initiator of cardiovascular risk and disease (3, 33).

Elastin endows large arteries, which experience substantial cyclic distensions, with a significant passive elastic recoil that promotes flow during diastole; proteoglycans provide some viscous dissipation; and fibrillar collagen provides stiffness that protects smooth muscle cells from acute overextension during pressurization and thereby preserves contractility (9). The magnitude of arterial pulsations results from a complex interplay of wall properties, downstream resistances, and reflected waves and thus varies with location along the vascular tree (33). Endothelial cells, smooth muscle cells, and fibroblasts sense altered hemodynamics directly or indirectly and modify the organization, synthesis, and degradation of structurally significant constituents within the ECM to restore, within a tolerance, intramural and wall shear stresses toward normal (4, 15, 18). Cyclic stimulation can greatly influence this relationship by modulating cellular differentiation status (37), including associated production/removal of matrix (7, 11, 19, 26, 40). This phenomenon has been well documented in vitro by subjecting cultured vascular cells to static vs. cyclic stretching (19, 20, 26, 40, 42) but has not been explored fully in vivo, where three-dimensional cell-cell and cell-ECM matrix interactions are important (11).

We previously showed that mouse carotid arteries exhibit a significant growth and remodeling response that correlates better with pulsatile than mean stimuli 35 to 56 days after an aortic banding-induced hypertension (7). There is a pressing need, however, to understand better the early time course of such responses, that is, to quantify how wall structure and properties evolve over days or weeks to optimize long-term function over the cardiac cycle. Such information will also prove essential in the development of predictive mathematical models of arterial disease that promise to improve interventional planning. In this study, we examine the hypotheses that marked carotid artery remodeling occurs within the first 1–2 wk following an abrupt but sustained increase in pulse pressure and that associated changes in ECM are mediated in part by a local upregulation of monocyte chemoattractant protein-1 (MCP-1). Toward this end, we quantified changes in morphology, histology, and biomechanics 0, 7, 10, 14, or 42 days after pulse pressure was increased in the right common carotid artery by placing a constrictive band on the aortic arch just distal to the innominate artery.

METHODS

The Texas A&M Institutional Animal Care and Use Committee approved all surgical and experimental protocols, details of which are

Address for reprint requests and other correspondence: J. D. Humphrey, Dept. of Biomedical Engineering, Malone Engineering Center, Yale Univ., 55 Prospect St., New Haven, CT 06520-8260 (e-mail: jay.humphrey@yale.edu).

 0363-6135/10 Copyright © 2010 the American Physiological Society

provided in Eberth et al. (7). Briefly, transverse aortic arch banding surgery was performed, at 9–10 wk of age, on wild-type male mice having a hybrid C57BL/6J and 129Sv background. A constant-diameter (~400 μm) ligature (or band) was secured around the aorta between the innominate and left common carotid arteries to reduce locally both the compliance and lumen within the aortic arch. This surgical procedure forces a reflected periodic pressure wave through the right common carotid artery, thus increasing its pulsatile pressure and flow while maintaining nearly the same mean values as in the left common carotid (22); this increased pulsatility on the right side was evident immediately after banding. Mice were then allowed to recover for 0, 7, 10, 14, or 42 days after surgery, at which time a tail-cuff transducer was used to measure blood pressure, ultrasound was used to measure blood velocities in both common carotid arteries as well as within the aortic constriction, and the carotids were excised for in vitro biaxial testing and subsequent histology.

The pulsatility index (PI), a normalized metric of pulsatile blood velocity, was calculated from velocity measurements in the carotids, namely $PI = (V_{max} - V_{min})/V_{mean}$, where V is velocity (12). Blood pressures were estimated in the left carotid via Poiseuille's relation, and the pressure was measured via the tail cuff; verified relations for a pressure drop across a stenosis were then used to estimate pressures in the right carotid (22). In vitro biaxial mechanical tests were performed on the excised, paired carotid arteries from each mouse with the use of a custom mechanical test system (10), and pressure-diameter/axial force-length data were collected during cyclic pressurization (from 0 to 140 mmHg) and axial extension (from 0 to 8.8 mN loading) protocols under basal smooth muscle tone. Overall smooth muscle and endothelial cell function were then evaluated at constant pressure (80 mmHg) and axial extension (individual in vivo value) using function testing protocols outlined in Eberth et al. (8); that is, time-dependent changes in diameter at constant pressure in response to 10^{-5} M phenylephrine and then 10^{-5} M sodium nitroprusside. Only those vessels that retained at least minimal function (i.e., >5% uniform change in diameter after dosage with vasoreactants) were included in the data analysis. Preliminary studies suggested that both nonuniform constriction/dilation and complete loss of smooth muscle or endothelial response were due primarily to excessive stretching during excision, mounting, or mechanical testing, which occurred in 12.3% of all vessels. Finally, histology was performed using cross sections stained with hematoxylin and eosin (H&E), Verhoeff-Van Gieson (VVG), Picro-Sirius red (PSR), or Safranin-O and quantified with computer-aided Hue-Saturation-Luminescence (HSL) thresholding (cf. Ref. 13). The ratio of monocyte chemoattractant protein-1 (MCP-1) to elastin was quantified (7) using an anti-MCP-1 antibody (green fluorescence) and elastin (red) autofluorescence.

Data from right and left common carotid arteries 7, 10, 14, or 42 days after banding (RCCA-B and LCCA-B, respectively) were compared either at a particular end point or relative to data from *day 0* baseline common carotid arteries (CCA). Overall, 42 arteries were studied from 21 mice ($n = 4–5$ per group). Outliers were removed from hemodynamic and arterial wall measurements using the quartile method. Prior findings demonstrated significant long-term changes, relative to baseline controls, due to increased pulse pressure in this mouse model (7). Time course data reported by Xu et al. (41) and Hu et al. (13), based on descending thoracic aorta coarctation models in other species, suggest, however, that significant remodeling may occur within the first 2 wk following surgery. Hence, our focus was to compare expected differences in remodeling responses by RCCA-B and LCCA-B at early end points, namely, 7, 10, and 14 days following banding surgery. Comparisons of hemodynamic, mechanical, and histological metrics were considered statistically significant when $P < 0.05$, with P calculated based on the Student's t distribution using $n - 2$ degrees of freedom and two tails.

RESULTS

Mean arterial pressure (MAP) was virtually identical (98.1 ± 4.44 mmHg) for the right and left carotids at *day 0* (dotted line in Fig. 1*A*) and did not change markedly in either side over the 42 days following banding. Diastolic pressure did not change much in RCCA-B but dropped slightly in LCCA-B. Systolic pressure increased significantly at *day 7* in RCCA-B (147 ± 0.616 mmHg) compared with CCA (120 ± 1.91 mmHg), reached a peak at *day 14* (154 ± 8.42 mmHg), and returned toward baseline at *day 42* (124 ± 10.3 mmHg). Meanwhile, the LCCA-B did not experience substantial changes in systolic pressure except for a slight decrease at *day 42* after banding (110 ± 1.02 mmHg). Accordingly, the pulse pressure in the right carotid was significantly higher 7 days after banding (CCA, 43.0 ± 4.08; RCCA-B, 79.7 ± 4.01; LCCA-B, 42.6 ± 2.44 mmHg) and remained higher than baseline thereafter (Fig. 1*B*). Mean volumetric flow rate (Q_{mean}) nearly doubled at *day 7* in the right, but not the left, carotid (CCA, 0.016 ± 0.003; RCCA-B, 0.032 ± 0.001; LCCA-B, 0.021 ± 0.005 ml/s) but then returned toward baseline (Fig. 2*A*). PI was always higher in the right than in the left carotid after banding (Fig. 2*B*).

Pressure-diameter testing at fixed axial extensions revealed a marked increase in the outer diameter of the RCCA-B; there

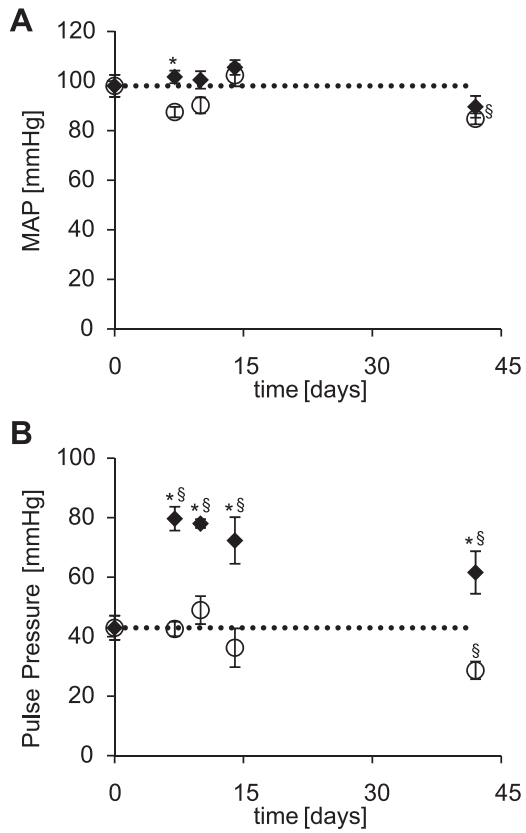

Fig. 1. Noninvasive in vivo measurements of mean arterial pressure (MAP; *A*) and pulse pressure (*B*). Data are shown for the right common carotid artery after banding (RCCA-B; ♦) and the left common carotid artery after banding (LCCA-B; ○), both of which were excised and studied further at multiple time points: at either *day 0* or *7*, *10*, *14*, or *42* days after banding surgery. Because *time 0* was before surgery, it represents the baseline common carotid artery (CCA) control, with the dotted line emphasizing the baseline values for comparative purposes. Values are means ± SE ($n = 4–7$). *$P < 0.05$, RCCA-B vs. LCCA-B. §$P < 0.05$, RCCA-B or LCCA-B vs. CCA.

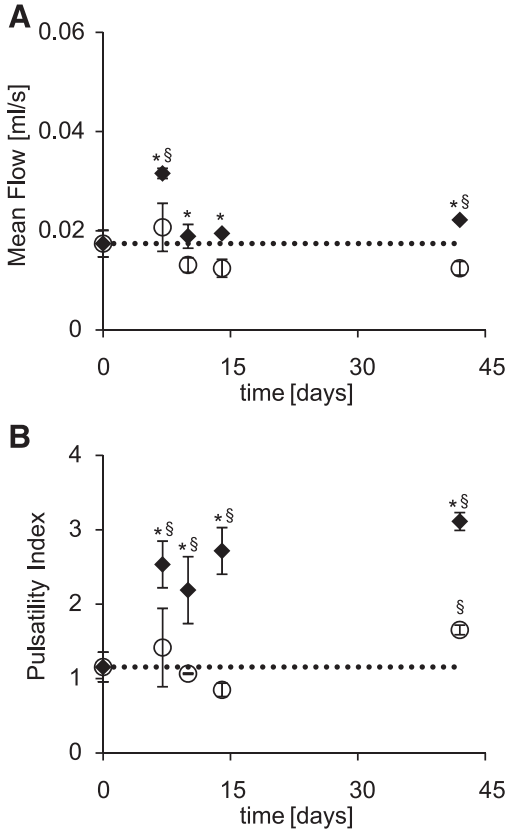

Fig. 2. Noninvasive in vivo measurement of mean blood flow (A) and pulsatility index (PI = $V_{max} - V_{min}/V_{mean}$, where V is velocity; B). Hence, data are for RCCA-B (♦) and LCCA-B (○) at each time point: 0, 7, 10, 14, or 42 days after banding surgery. Because *time 0* was before surgery, it represents the baseline CCA (dotted line). Values are means ± SE (n = 4–7). *$P < 0.05$, RCCA-B vs. LCCA-B. §$P < 0.05$, RCCA-B or LCCA-B vs. CCA.

was, however, a slight decrease in outer diameter following its peak at *day 14* (Fig. 3*A*). The LCCA-B had a modest increase in outer diameter, with a similar slight decrease after *day 14*. Axial force-length testing revealed dramatic increases in force for a given axial stretch as time progressed from 0 to 42 days in the RCCA-B but little to no change in the LCCA-B (Fig. 3*B*). RCCA-B axial force-stretch data were similar from 14 to 42 days, thus revealing that most changes occurred on or before *day 14*. LCCA-B data were similar at all times after banding and did not differ significantly from those of the CCA. There was a significant decrease in the in vivo axial stretch (λ_z^{iv}) for the RCCA-B (Fig. 3*B*); it reached a minimum at *day 14* (1.18 ± 0.067) and remained low at *day 42*. In contrast, λ_z^{iv} for the LCCA-B changed little (e.g., 1.67 ± 0.040) after banding.

Wall thickness of the banded vessels increased gradually during the first 10 days (CCA, 24.8 ± 0.878; RCCA-B, 46.1 ± 0.531; LCCA-B, 42.0 ± 1.52 μm) but increased dramatically in the RCCA-B at *day 14* (99.0 ± 8.43 μm) and remained high (Fig. 4*A*). The inner diameter (Fig. 4*B*) of the RCCA-B measured at MAP also peaked at *day 14* (680 ± 32.0 μm) and then decreased slightly at *day 42*; in comparison, the inner diameter of the CCA was 484 ± 8.51 μm at MAP. Conversely, the inner diameter of the LCCA-B fluctuated with an apparent mean value of 507 μm and range of 72.3 μm. The ratio of the fully passive to active diameter is a measure of the overall contractile capacity of the vessel. This ratio was determined by adding a vasoconstrictor (phenylephrine 10^{-5} M) and then a vasodilator (sodium nitroprusside 10^{-5} M) to the adventitial bath while the vessels were pressurized at 80 mmHg and held at their individual in vivo axial stretch. For example, the passive to active diameter ratios were 1.62 ± 0.02 in the CCA, 1.15 ± 0.04 in the RCCA-B, and 1.59 ± 0.01 in the LCCA-B at *day 14*. The number of cell nuclei stained using H&E (Fig. 4*C*) revealed an initially gradual but then significant increase in nuclei number for RCCA-B, whereas that for LCCA-B remained nearly the same over the 42-day study period (CCA, 298 ± 58.9; RCCA-B, 578 ± 28.3; LCCA-B, 264 ± 39.5 nuclei).

Figure 5*A* shows circumferential stress-stretch data for all three groups of vessels at each time postsurgery for pressurizations from 0 to 140 mmHg at the individual in vivo axial stretches; Fig. 5*B* shows similar axial stress-stretch data. Behaviors were qualitatively similar in the circumferential direction at all times among the three groups. Conversely, the axial stress-stretch data revealed an increase in axial stress for any given axial stretch in the high-pulsatility vessels compared with that found in the low-pulsatility or baseline vessels; this pattern increased with time (cf. Fig. 3*B*).

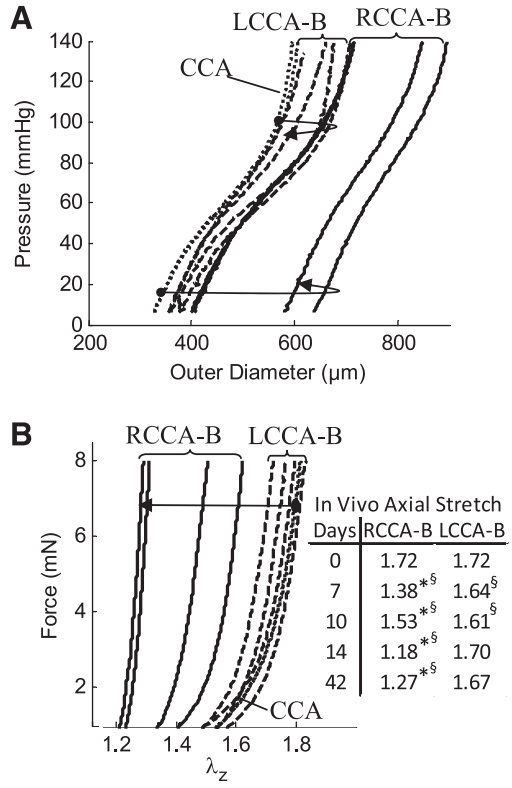

Fig. 3. Data from in vitro biaxial mechanical tests for cyclic pressurization protocols at a fixed length (*A*; i.e., pressure-outer diameter data at in vivo axial stretch, λ_z^{iv}) and cyclic extension protocols at a fixed pressure (*B*; i.e., axial force-stretch data at 100 mmHg). The measured in vivo axial stretch is tabulated in Fig. 3*B* with an SE <0.03 for all values. For the in vivo axial stretch: *$P < 0.05$, RCCA-B vs. LCCA-B. §$P < 0.05$, RCCA-B or LCCA-B vs. CCA. Values and curves are shown at each time point: 0 (CCA, dotted lines) or 7, 10, 14, or 42 days after banding surgery for both RCCA-B (solid lines) and LCCA-B (dashed lines). Arrows show shifts in diameter or force as time increased, indicating a maximal outer diameter for both vessels at *day 14* and force at *day 42*.

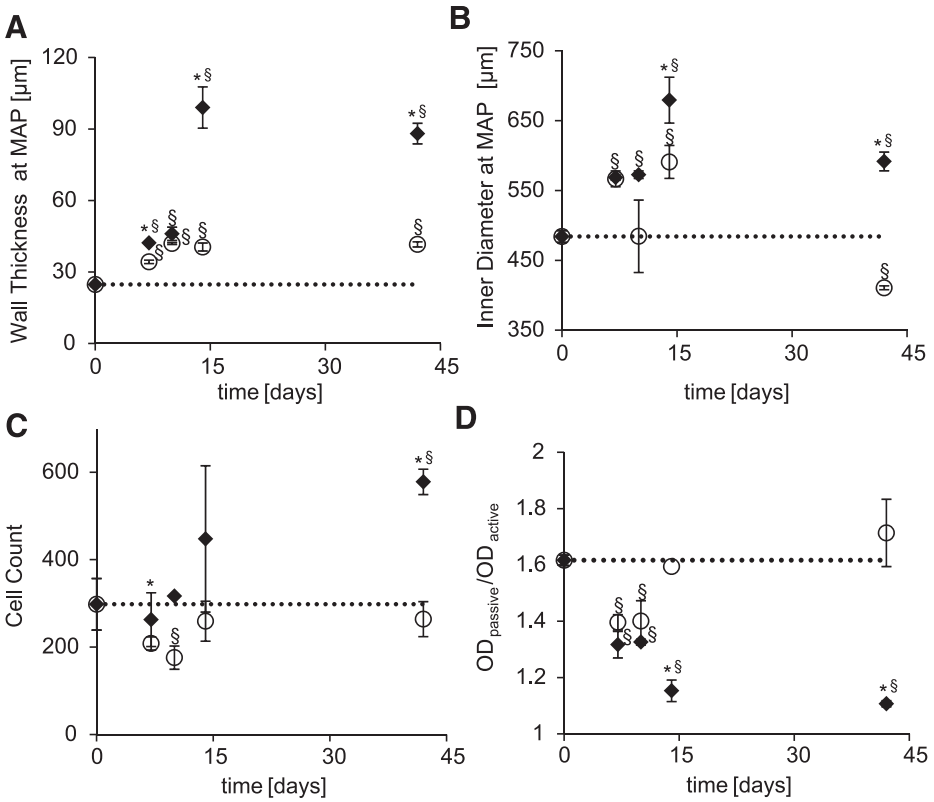

Fig. 4. Morphological metrics: wall thickness (*A*), inner diameter (*B*), cell count from the hematoxylin and eosin stain (*C*), and endothelium-independent ratio of passive to active outer diameter at 100 mmHg (*D*). Data are shown for the RCCA-B (♦) and LCCA-B (○) at each time point: 0, 7, 10, 14, or 42 days after banding surgery. Note that *time 0* is before surgery and thus represents the baseline CCA (dotted line). Values are means ± SE. *$P < 0.05$, RCCA-B vs. LCCA-B. §$P < 0.05$, RCCA-B or LCCA-B vs. CCA.

Representative histological results obtained from VVG- and PSR-stained sections can be seen in Fig. 6 (normal and polarized light, respectively). VVG-stained tissue (Fig. 6, *a–i*) shows elastin as black and collagen/smooth muscle as pink, which can be compared with the PSR-stained tissue (Fig. 6, *j–r*) that reveals collagen as birefringent. Columns compare representative RCCA-B and LCCA-B (1 per group) at each end point after banding. Thresholding analysis of VVG-stained tissue showed little change in elastin area fraction (ϕ^e) in the LCCA-B over the 42 days postsurgery, whereas the RCCA-B experienced a gradual reduction (Fig. 6*s*). This decrease in elastin area fraction in the RCCA-B was due in large part to a large increase in collagen area fraction ϕ^c, particularly at *day 42* [CCA, 0.223 ± 0.056; RCCA-B, 0.314 ± 0.011; LCCA-B, 0.257 ± 0.002 (7)] with no significant change for the LCCA-B (Fig. 6*t*). Representative histological results obtained from Safranin-O-stained sections at each end point are shown in Fig. 7, *a–i*, with quantification of the area fraction of glycosaminoglycans (GAGs) to vessel cross-sectional area shown in Fig. 7*s*. Note the consistently elevated GAG content in the right carotid arteries after banding, peaking at *day 14*, compared with the left. Immunostaining for MCP-1 with overlaid elastin autofluorescence (Fig. 7, *j–r*) revealed a steady increase in MCP-1-to-elastin ratio in the highly pulsatile right side (Fig. 7*t*). The left side had a modest short-term inflammatory response, highest at 7 days.

DISCUSSION

Hypertension causes, and is caused by, marked changes in the structure and function of blood vessels, the most conspicuous of which are typically an increase in wall thickness and a reduction in compliance (which reflects altered pressure-diameter responses). Nevertheless, there is little information on the relative time courses of such changes, particularly during early periods of disease progression, and no detailed correlations with corresponding measures of blood pressure and flow. Among the many findings in this study, particularly novel ones include the following: *1*) one of the earliest marked changes in the right carotid artery (by *day 7*) was a reduction in the in vivo axial stretch, with an associated increase in axial stiffness that reached steady state by 14 days; *2*) there was an early and marked endothelial independent reduction in overall contractile capacity (by *day 7*), which also reached steady state by *day 14*; *3*) modest increases in wall thickness over the first 10 days were followed by a dramatic "over" thickening (between *days 10* and *14*) that decreased slightly by 42 days; *4*) modest increases in intramural cell number over the first 10 days were followed by a dramatic increase by *day 14* (primarily in the adventitia) that continued slowly thereafter to 42 days; and *5*) much of the adventitial collagen produced between *days 10* and *14* was organized loosely, with an apparent slight compaction thereafter (at 42 days). Note, too, that inner diameter increased to its peak at 14 days despite the transient increase in mean flow peaking much earlier (on or before *day 7*) and the PI remaining significantly elevated over the entire 42-day study. Finally, MCP-1 was upregulated in both the media and adventitia in the right carotid, particularly on *day 14* and beyond. Whereas our earlier study of carotid adaptation in this banding model (7) looked at long-term effects of hypertension (5–8 wk), the present findings demonstrate a complex early time course in the multiaxial changes, with the first 2 wk following the abrupt onset of increased pulsatility representing a critical transition period for much of the growth and remodeling.

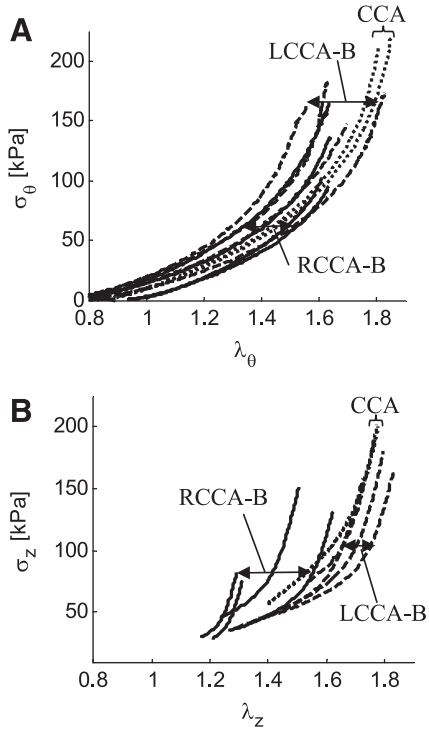

Fig. 5. Mean circumferential (*A*) and axial stress-stretch behaviors (*B*) at each time point: 0 (CCA; dotted lines) and 7, 10, 14, or 42 days after banding surgery for both RCCA-B (solid lines) and LCCA-B (dashed lines). Note that to encourage vessel viability based on other experiments in our laboratory (7, 8), an 8.8 mN force transducer limit was enforced throughout testing. The RCCA-B reached the force transducer limit at lower axial stretch (cf. Fig. 3*B*); thus calculated axial stresses do not reach levels comparable to those found in the CCA and LCCA-B.

The transverse aortic arch banding model is a convenient method to separate effects of mean and pulse pressure (cf. Fig. 1), with the abrupt marked increase in pulse pressure in the right carotid (e.g., 79.7 ± 4.02 mmHg at *day 7* relative to 43.0 ± 4.08 mmHg at baseline) continuing over many weeks despite a slight decrease (to 61.6 ± 7.14 mmHg) at *day 42*. These findings are similar to but extend those of Rockman et al. (30), who showed an increase in systolic pressure for the duration of their banding study (7 days), and those of Nakamura et al. (25), who showed increases in systolic pressure around *day 3*. In addition, the right carotid experienced a large increase in pulsatility index, beginning by *day 7* after banding, despite an almost normal mean flow on all days except *day 7*. Li et al. (22) similarly reported that mean velocities remained comparable between the right and left carotids after banding surgery. Restoration of the mean volumetric flow rate in the right carotid to near baseline by *day 10* suggested a similarly rapid regulatory response by smaller, distal vessels (21). Guyton and Hartley (12) showed that inner diameter correlated strongly with peak flow velocity and pulsatile, not mean, flow in a rat model of reduced carotid flow following a recovery period of 39–82 days. Although we similarly found a stronger correlation between inner diameter and PI vs. mean flow at long times, the latter was still significant (7). Indeed, that inner diameter decreased slightly after *day 14* despite the continued elevation in PI (cf. Figs. 2 and 4) suggests the need to delineate further the complex roles of mean and pulsatile flow on arterial responses.

Our findings demonstrate a rapid local growth and remodeling response, with most changes occurring within the first 14 days (cf. Fig. 4, *A* and *B*). Many investigators believe that the cascade of arterial responses to altered hemodynamics starts with the endothelial cells, followed thereafter by the smooth muscle cells and fibroblasts. For example, endothelial responses to altered wall shear stress (e.g., altered production of nitric oxide and endothelin-1) can be rapid (4, 5), which in turn induces rapid changes in smooth muscle contractility that can be followed by subsequent alterations in the production of growth factors and proteases that aid in structural remodeling, including significant deposition of collagen (15, 31). Regardless, two of the earliest marked tissue-level changes (by *day 7*) were changes in axial stretch and stiffness as well as endothelium-independent contractility. There is clearly a need to determine the relative roles of the different types of vascular cells in these early responses. Finally, we emphasize that the marked, continual increase in MCP-1 (Fig. 7*t*) implicates the importance of cyclic wall stretch/stress in promoting local inflammation in this mechanically induced model of hypertension.

Although it is widely held that arteries increase or decrease wall thickness and caliber in an attempt to maintain both intramural and wall shear stress near homeostatic values (4, 15, 18), in both our earlier (7) and this present study, the calculated intramural stresses in the right carotid increased abruptly due to banding but then decreased well below baseline. This finding is seen easily at all end points by combining pressure, radius, and thickness data [$\sigma_\theta = P \cdot r_i/(r_o - r_i)$, where P is pressure and r_i and r_o are inner and outer radius; cf. Figs. 1*A* and Fig. 4, *A* and *B*]. It is possible that excessive production of nontensile bearing wall constituents, including GAGs and reticular collagens (cf. Figs. 6 and 7), may have contributed to the early excessive thickening and functioned, in part, to increase viscous dissipation in response to the cyclic loading. It is well known, for example, that cyclic stimulation of vascular cells in culture generally upregulates growth factors (e.g., TGF-β, PDGF, and FGF) and thereby the associated synthesis of structural proteins and glycoproteins (11, 26, 40). Indeed, Walker-Caprioglio et al. (39) reported that proteoglycan synthesis increases in arteries in a spontaneously hypertensive rat model, particularly in carotids, and Reynertson et al. (29) reported similar findings in the aorta. Similar findings also have been seen in cell culture. Collagen mass fraction (ϕ^c) was also increased greatly by 14 days herein, similar to that found by Hu et al. (13) in a mini-pig aortic coarctation model, and remained high over the study period. As shown in Figs. 6 and 4, however, the loose and poorly organized collagen that was produced between *days 10* and *14* appeared to be compacted slightly by *day 42*. This novel observation may suggest that collagen remodeling was not complete even at 42 days and that initially synthesized and deposited collagen (and GAGs) may be reorganized subsequently to increase its load-bearing efficiency.

Whereas it has long been thought that hypertension initially increases wall stress primarily in the inner portion of the wall (24), thus leading first to a medial or subintimal remodeling that is presumably controlled by smooth muscle cells (24), the significant remodeling observed in the present study in the adventitia is consistent with numerous reports on the impor-

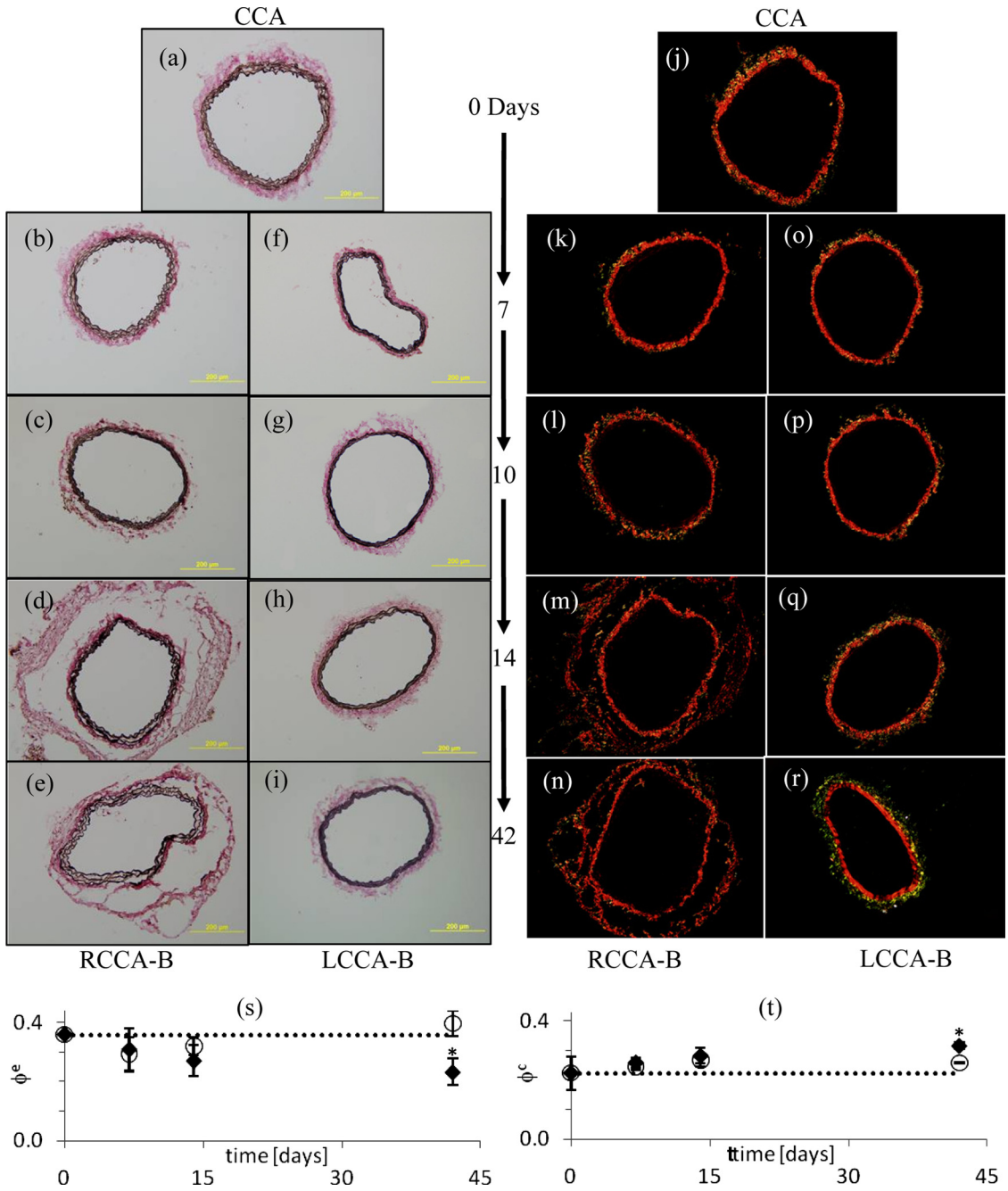

Fig. 6. Representative histological images of RCCA-B and LCCA-B at 0, 7, 10, 14, and 42 days after aortic banding surgery using Verhoeff-Van Gieson (VVG; *a–i*) to show elastin in black and Picro-Sirius red (PSR; *j–r*) multicolored collagen shown through birefringence. Quantified results are presented as elastin area fraction (ϕ^e; *s*) and collagen area fraction (ϕ^c; *t*) for the RCCA-B (♦) and LCCA-B (○) at each time point: 0, 7, 10, 14, or 42 days after banding surgery. Values are means ± SE. *$P < 0.05$, RCCA-B vs. LCCA-B.

tance of adventitial remodeling (23, 28, 34, 36). Indeed, 69% of the cell nuclei at *day 42* were within the adventitia of the hypertensive RCCA-B compared with 26% in the contralateral LCCA-B (7). These findings highlight the need to delineate potentially different roles of smooth muscle cells and fibroblasts in hypertensive remodeling and whether these two different cell types respond to the same extents of altered cyclic stimuli or seek to restore the same metrics toward the same or different homeostatic targets. Our findings of a persistent, gradual increase in MCP-1 in the RCCA-B (Fig. 7*t*) also revealed that much of its activity was focused in the adventitia (Fig. 7, *j–r*). This finding is consistent with suggestions that the adventitia is a site of "injury sensing" and "inflammation signaling" (35, 38), as well as being potentially important in the development of atherosclerosis (32).

Although we did not track directly the time course of potential phenotypic modulation of the smooth muscle cells, the available contractile range for regulating arterial diameter was significantly less in the RCCA-B than in the CCA and LCCA-B at *days 14* and *42* (Fig. 4*D*). Hu et al. (13) reported

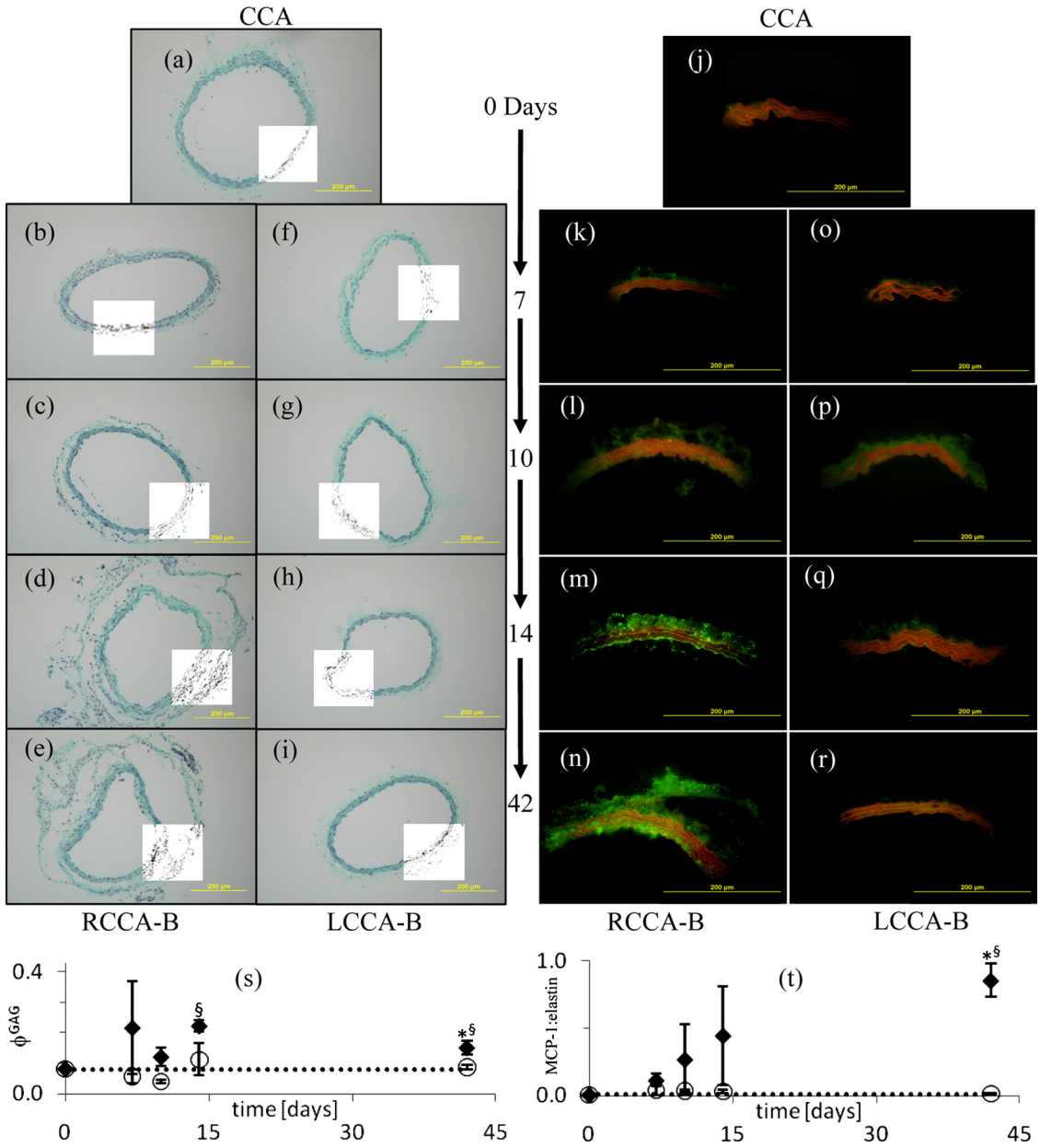

Fig. 7. Representative histological and immunohistochemical images of RCCA-B and LCCA-B at 0, 7, 10, 14, and 42 days after aortic banding surgery using Safranin-O stain (*a–i*) to visualize glycosaminoglycans [GAG; H = 173–240°, S = 0.09–0.16, L = 0.1–0.8 (7), with superimposed positive thresholding pixels shown in black within the *insets*], and overlaid and zoomed (different length scale than in Fig. 6) monocyte chemoattractant protein-1 (MCP-1; *j–r*) fluorescence (green) and elastin autofluorescence (red). Thresholding results for GAG area fraction (ϕ^{GAG}; *s*) and the ratio of MCP-1 to elastin (*t*). Data are shown for the RCCA-B (♦) and LCCA-B (○) at each time point: 0, 7, 10, 14, or 42 days after banding surgery. Values are means ± SE. *$P < 0.05$, RCCA-B vs. LCCA-B. §$P < 0.05$, RCCA-B or LCCA-B vs. CCA.

a parallel decrease in contractile phenotype and shift toward a synthetic phenotype by aortic smooth muscle cells (measured via immunohistochemistry), with attendant increases in procollagen production peaking at 2 wk during an 8-wk study period in a suprarenal aortic coarctation model in the mini-pig; they also reported peak smooth muscle cell proliferation at 2 wk. The rate of cell proliferation may have similarly been highest at *day 14* and leveled off by *day 42* in our study.

Noting that the arterial wall is subjected to coupled biaxial stretches and stresses in vivo, recall that the in vivo axial stretch decreased rapidly and dramatically in the RCCA-B (Fig. 3*B*). It has been proposed that arteries may use the axial direction to complement circumferential remodeling and thereby achieve balanced changes in wall shear and intramural stresses (16). The force required to maintain an artery at its in vivo stretch depends greatly on intramural elastin (6), which exhibited a decreased mass fraction in the present study (cf. Fig. 6) consistent with well-known changes in hypertension and aging (1, 17, 27). It would be interesting to determine whether the elastin became increasingly fragmented, further reducing its load-carrying capability. Regardless, it is now clear that axial remodeling (at the tissue level) is one of the early responses to an abrupt increase in pulsatility and thus merits increased attention. Indeed, the structural stiffness of the

arterial wall is determined by many factors, including the multiaxial state of stress; hence, even the increased attention in hypertension research to metrics such as pulse wave velocity (1, 17, 27) should consider possible changes in axial properties.

We submit that the transverse aortic banding model, by altering pulsatile pressure and flow without significantly affecting mean values, is a valuable animal model to study arterial growth and remodeling in response to hypertension, perhaps with greatest application to understanding effects of isolated systolic and aging-related hypertension wherein pulse pressure plays a key role. Similar studies addressing possible differences in the time course of remodeling in male vs. female mice would be of particular interest, as would studies in atheroprone (e.g., ApoE$^{-/-}$) mice, particularly given the importance of hypertension in the possible rupture of vulnerable plaques in carotids that lead to stroke. Finally, better identification of molecular mechanisms underlying changes in cellular distribution, phenotypic modulation, and extracellular matrix organization in response to pulsatile hemodynamics promises to not only increase our understanding of the evolution of the arterial wall in hypertension but also provide the information needed to mathematically model this process and thereby gain more predictive capability (15).

ACKNOWLEDGMENTS

We thank Dr. Anil Reddy, Jaclyn Boone, and Jan Eberth for technical guidance.

GRANTS

This research was supported, in part, by National Heart, Lung, and Blood Institute Grant HL-64372 through the Bioengineering Research Partnership Program.

DISCLOSURES

No conflicts of interest, financial or otherwise, are declared by the author(s).

REFERENCES

1. **Arribas SM, Hinek A, Gonzalez MC.** Elastic fibres and vascular structure in hypertension. *Pharmacol Ther* 111: 771–791, 2006.
2. **Berne RM, Levy MN.** *Cardiovascular Physiology*. St. Louis, MO: Mosby, 2001.
3. **Boutouyrie P, Bussy C, Lacolley P, Girerd X, Laloux B, Laurent S.** Association between local pulse pressure, mean blood pressure, and large-artery remodeling. *Circulation* 100: 1387–1393, 1999.
4. **Chien S.** Effects of disturbed flow on endothelial cells. *Ann Biomed Eng* 36: 554–562, 2008.
5. **Davies PF.** Hemodynamic shear stress and the endothelium in cardiovascular pathophysiology. *Nat Clin Pract Cardiovasc Med* 6: 16–26, 2009.
6. **Dobrin PB, Schwarcz TH, Mrkvicka R.** Longitudinal retractive force in pressurized dog and human arteries. *J Surg Res* 48: 116–120, 1990.
7. **Eberth JF, Gresham VC, Reddy AK, Popovic N, Wilson E, Humphrey JD.** Importance of pulsatility in hypertensive carotid artery growth and remodeling. *J Hypertens* 27: 2010–2021, 2009.
8. **Eberth JF, Taucer AI, Wilson E, Humphrey JD.** Mechanics of carotid arteries in a mouse model of Marfan Syndrome. *Ann Biomed Eng* 37: 1093–1104, 2009.
9. **Faury G.** Function-structure relationship of elastic arteries in evolution: from microfibrils to elastin and elastic fibres. *Pathol Biol (Paris)* 49: 310–325, 2001.
10. **Gleason RL, Gray SP, Wilson E, Humphrey JD.** A multiaxial computer-controlled organ culture and biomechanical device for mouse carotid arteries. *J Biomech Eng* 126: 787–795, 2004.
11. **Gupta V, Grande-Allen KJ.** Effects of static and cyclic loading in regulating extracellular matrix synthesis by cardiovascular cells. *Cardiovasc Res* 72: 375–383, 2006.
12. **Guyton JR, Hartley CJ.** Flow restriction of one carotid artery in juvenile rats inhibits growth of arterial diameter. *Am J Physiol Heart Circ Physiol* 248: H540–H546, 1985.
13. **Hu JJ, Ambrus A, Fossum TW, Miller MW, Humphrey JD, Wilson E.** Time courses of growth and remodeling of porcine aortic media during hypertension: a quantitative immunohistochemical examination. *J Histochem Cytochem* 56: 359–370, 2008.
14. **Humphrey JD.** *Cardiovascular Solid Mechanics: Cells, Tissues, and Organs*. New York: Springer, 2002, p. xvi.
15. **Humphrey JD.** Vascular adaptation and mechanical homeostasis at tissue, cellular, and sub-cellular levels. *Cell Biochem Biophys* 50: 53–78, 2008.
16. **Humphrey JD, Eberth JF, Dye WW, Gleason RL.** Fundamental role of axial stress in compensatory adaptations by arteries. *J Biomech* 42: 1–8, 2009.
17. **Lakatta EG, Wang M, Najjar SS.** Arterial aging and subclinical arterial disease are fundamentally intertwined at macroscopic and molecular levels. *Med Clin North Am* 93: 583–604, 2009.
18. **Langille BL.** Arterial remodeling: relation to hemodynamics. *Can J Physiol Pharmacol* 74: 834–841, 1996.
19. **Leung DY, Glagov S, Mathews MB.** Cyclic stretching stimulates synthesis of matrix components by arterial smooth muscle cells in vitro. *Science* 191: 475–477, 1976.
20. **Li Q, Muragaki Y, Hatamura I, Ueno H, Ooshima A.** Stretch-induced collagen synthesis in cultured smooth muscle cells from rabbit aortic media and a possible involvement of angiotensin II and transforming growth factor-beta. *J Vasc Res* 35: 93–103, 1998.
21. **Li YH, Reddy AK, Ochoa LN, Pham TT, Hartley CJ, Michael LH, Entman ML, Taffet GE.** Effect of age on peripheral vascular response to transverse aortic banding in mice. *J Gerontol A Biol Sci Med Sci* 58: B895–B899, 2003.
22. **Li YH, Reddy AK, Taffet GE, Michael LH, Entman ML, Hartley CJ.** Doppler evaluation of peripheral vascular adaptations to transverse aortic banding in mice. *Ultrasound Med Biol* 29: 1281–1289, 2003.
23. **Maiellaro K, Taylor WR.** The role of the adventitia in vascular inflammation. *Cardiovasc Res* 75: 640–648, 2007.
24. **Matsumoto T, Hayashi K.** Mechanical and dimensional adaptation of rat aorta to hypertension. *J Biomech Eng* 116: 278–283, 1994.
25. **Nakamura A, Rokosh DG, Paccanaro M, Yee RR, Simpson PC, Grossman W, Foster E.** LV systolic performance improves with development of hypertrophy after transverse aortic constriction in mice. *Am J Physiol Heart Circ Physiol* 281: H1104–H1112, 2001.
26. **O'Callaghan CJ, Williams B.** Mechanical strain-induced extracellular matrix production by human vascular smooth muscle cells: role of TGF-beta(1). *Hypertension* 36: 319–324, 2000.
27. **O'Rourke MF, Hashimoto J.** Mechanical factors in arterial aging: a clinical perspective. *J Am Coll Cardiol* 50: 1–13, 2007.
28. **Pagano PJ, Gutterman DD.** The adventitia: the outs and ins of vascular disease. *Cardiovasc Res* 75: 636–639, 2007.
29. **Reynertson RH, Parmley RT, Roden L, Oparil S.** Proteoglycans and hypertension. I. A biochemical and ultrastructural study of aorta glycosaminoglycans in spontaneously hypertensive rats. *Coll Relat Res* 6: 77–101, 1986.
30. **Rockman HA, Knowlton KK, Ross JJ, Chien KR.** In vivo murine cardiac hypertrophy: a novel model to identify genetic signaling mechanisms that activate an adaptive physiological response. *Circulation* 87: VII-14–VII-21, 1993.
31. **Rodriguez-Feo JA, Sluijter JP, de Kleijn DP, Pasterkamp G.** Modulation of collagen turnover in cardiovascular disease. *Curr Pharm Des* 11: 2501–2514, 2005.
32. **Ross R.** Atherosclerosis—an inflammatory disease. *N Engl J Med* 340: 115–126, 1999.
33. **Safar ME, Boudier HS.** Vascular development, pulse pressure, and the mechanisms of hypertension. *Hypertension* 46: 205–209, 2005.
34. **Sartore S, Chiavegato A, Faggin E, Franch R, Puato M, Ausoni S, Pauletto P.** Contribution of adventitial fibroblasts to neointima formation and vascular remodeling: from innocent bystander to active participant. *Circ Res* 89: 1111–1121, 2001.
35. **Stenmark KR, Davie N, Frid M, Gerasimovskaya E, Das M.** Role of the adventitia in pulmonary vascular remodeling. *Physiology (Bethesda)* 21: 134–145, 2006.
36. **Strauss BH, Rabinovitch M.** Adventitial fibroblasts: defining a role in vessel wall remodeling. *Am J Respir Cell Mol Biol* 22: 1–3, 2000.
37. **Sumpio BE, Banes AJ.** Response of porcine aortic smooth muscle cells to cyclic tensional deformation in culture. *J Surg Res* 44: 696–701, 1988.

38. **Wagenseil JE, Mecham RP.** Vascular extracellular matrix and arterial mechanics. *Physiol Rev* 89: 957–989, 2009.
39. **Walker-Caprioglio HM, Koob TJ, McGuffee LJ.** Proteoglycan synthesis in normotensive and spontaneously hypertensive rat arteries in vitro. *Matrix* 12: 308–320, 1992.
40. **Wilson E, Mai Q, Sudhir K, Weiss RH, Ives HE.** Mechanical strain induces growth of vascular smooth muscle cells via autocrine action of PDGF. *J Cell Biol* 123: 741–747, 1993.
41. **Xu C, Zarins CK, Bassiouny HS, Briggs WH, Reardon C, Glagov S.** Differential transmural distribution of gene expression for collagen types I and III proximal to aortic coarctation in the rabbit. *J Vasc Res* 37: 170–182, 2000.
42. **Ziegler T, Bouzourene K, Harrison VJ, Brunner HR, Hayoz D.** Influence of oscillatory and unidirectional flow environments on the expression of endothelin and nitric oxide synthase in cultured endothelial cells. *Arterioscler Thromb Vasc Biol* 18: 686–692, 1998.